

IONIZATION ALONG THE TRACKS OF HIGH-ENERGY ELECTRON-POSITRON PAIRS

A. A. VARFOLOMEEV, R. I. GERASIMOVA, L. A. MAKARINA, A. S. ROMANTSEVA, and S. A. CHUEVA

Submitted to JETP editor August 18, 1958

J. Exptl. Theoret. Phys. (U.S.S.R.) 36, 707-716 (March, 1959)

Experimental data are presented on the track densities of five high-energy electron-positron pairs in nuclear emulsions. The measurements were performed for the first pairs in electron-photon showers. The pair energy was estimated from the energy spectrum of cascade electrons at a distance of 2.5 or 3 radiation lengths from the vertex of the first pair. In three cases the pair energy was close to 10^{12} ev and in two cases was approximately 3×10^{11} ev. The track density was determined from grain density and from the gap length distribution. The track density of a pair near its vertex was found to be smaller than that of a particle for which the specific energy loss is twice as large as the ionization loss of an electron. This decrease of pair track density can be accounted for by the mutual electron-positron screening during the ionization process. The results are compared with the theoretical ionization curves for pairs calculated by Chudakov.

1. INTRODUCTION

WHEN an electron-positron pair is produced with energy greater than 10^{11} or 10^{12} ev a peculiar ionization effect is observed along the initial portion of the track. Before the separation between the electron and positron becomes greater than their range of interaction with electrons of the medium ($\sim 5 \times 10^{-7}$ cm) the specific ionization loss of the pair is less than twice the electron loss. The reduced ionization results from mutual screening of the electron and positron fields and was first calculated by Chudakov¹ as a function of the angle of divergence. Chudakov's result has since been confirmed by other investigators,^{2,3} who have shown that reduced ionization can actually be observed for pairs with $\gtrsim 10^{12}$ ev.

Grain density at the vertex of a pair increases with the ionization loss. When the separation of the electron and positron paths becomes $r \sim 5 \times 10^{-7}$ cm the grain density corresponds to that of particles with the double ionization loss $2I_{p1}$ (I_{p1} is the plateau value of the ionization). However, this level will not generally equal twice the track density of an electron with ionization loss I_{p1} because of the nonlinear relation between grain density and ionization.

The practical interest of the screening effect lies in the fact that the length of the track segment along which ionization continues to grow can in principle be used to determine the vertex angle, from which the energy quantum producing the pair can be calculated.^{4,5}

Lohrmann⁶ has shown that at distances greater

than $100 - 1000 \mu$ from the vertex the separation r of electron and positron tracks is determined mainly by multiple scattering. Therefore measurements to determine the vertex angle must be performed at distances from the vertex which are relatively uninfluenced by multiple scattering. At high energies, however, the tracks coalesce at such distances x from the vertex and it is impossible to determine the angle visually.

At a distance greater than 1 or 2 cm from the vertex of a high-energy pair the tracks of secondary pairs are usually observed and the energy of the pair may be considerably reduced by radiation loss. It thus becomes possible to measure multiple scattering directly along a relatively short track length. Since even the measurement of the relative amount of multiple scattering does not exclude the so called "grain noise" of emulsions ($\sim 0.10 \mu$) it is clear that pair energies can actually be determined from multiple scattering only at energies $\lesssim 10^{11}$ ev.

The screening effect can thus be used to determine pair energies in the high-energy range where the usual methods are no longer applicable. It is first necessary to determine the energy dependence of the effect, for which purpose both measurements of track densities and independent measurements of pair energies are required.

The present paper gives measurements of grain density and mean gap length along the tracks of five electron-positron pairs with energies $\gtrsim 3 \times 10^{11}$ ev. Pair energies were estimated from the energy spectrum of cascade electrons produced by the pair and track densities were measured

TABLE I

Designation of shower	Range in single emulsion layer, mm	Volume of stack, liters	Layer dimensions, cm	Emulsion type	Exposure altitude, km	Exposure time, hours
E-53	3.5	0.5	10×10	R-NIKFI	20	9.5
O-209	12	3.0	10×20	»	26	9
D-84	9	1.0	10×20	»	20	10
D-44	6.5	1.0	10×20	»	20	10
I-109	3	Part of stack I	13×13	Ilford G5		

over a few millimeters. Three pairs with $\sim 10^{12}$ ev revealed the screening effect. The results are in agreement with Chudakov's theoretical curves.¹

2. SHOWER CHARACTERISTICS

We studied electron-positron pairs which generated electron-photon showers in emulsions. Table I gives data on the emulsion stacks in which the showers were registered.⁷

The energies E_γ of pair-producing photons were determined from the energy spectrum of the cascade electrons. The method of determining E_γ was similar to that described by Pinkau⁸ and by Miesowicz et al.⁹

At distances of 2.5 or 3.0 radiation lengths from the vertex of the first pair the energy spectrum of electrons within 200–300 μ about the shower axis was measured from multiple scattering. (The total noise in measurements of second differences was 0.13 μ in a 250 μ cell.) Cascade curves were used to determine pair energies in first approximation from the number N of electrons with energies $> 3 \times 10^8$ ev. After corrections for the spatial distribution of electrons the same cascade curves were used to determine E_γ . We used Janossy's cascade curves;¹⁰ shower energies E_γ are given in Table II.

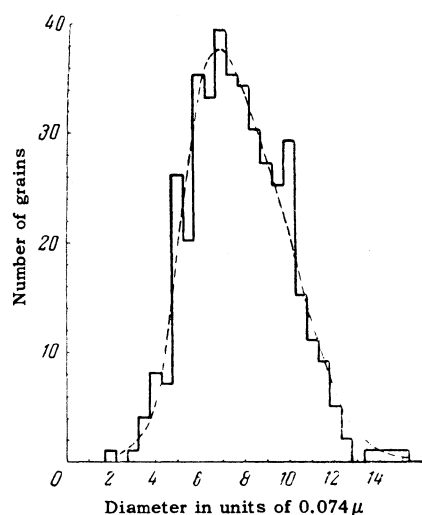


FIG. 1. Size distribution of developed grains in R-NIKFI emulsion. Mean diameter 0.57 μ .

TABLE II

Shower	E_γ (after Janossy), ev	E_γ (after Chudakov), ev
E-53	$(8.4^{+7.2}_{-5.1}) \cdot 10^{11}$	$2 \cdot 10^{12}$
O-209	$(1.0^{+0.62}_{-0.45}) \cdot 10^{12}$	$2 \cdot 10^{12}$
D-84	$(1.8^{+1.44}_{-0.92}) \cdot 10^{12}$	$2 \cdot 10^{12}$
D-44	$(3.3^{+2.6}_{-1.3}) \cdot 10^{11}$	
I-109	$(2.6^{+1.24}_{-0.98}) \cdot 10^{11}$	

The errors indicated in the table were determined from calculated data on fluctuations of N in a cascade. In accordance with Janossy's results¹² we determined the relative rms deviation σ from the mean value \bar{N} ($> \epsilon$). The experimental value of N was used to determine the mean value of E_γ , and the upper and lower limits of E_γ were determined from $N + \sigma N$ and $N - \sigma N$, respectively. We are now engaged in obtaining more accurate values of E_γ from curves calculated by the Monte Carlo method, taking into account the influence of the medium on bremsstrahlung;^{11,12} the results will be published at a later date.

3. CALIBRATION OF EMULSION

As can be seen from Table I, in the present work we used principally R-NIKFI (Motion Picture and Photography Research Institute) emulsions. Figure 1 gives the size distribution of developed silver grains in one of the emulsion stacks.

Pair track densities were determined in two ways. We first counted grains directly to determine the grain density n . The gap length distribution was also obtained. An exponential description of the integral distribution was determined by least squares, with the exponential index giving the mean gap length \bar{G} (Fowler and Perkins¹³). The procedure for measuring \bar{G} was simplified. Gap lengths were not measured; instead we only determined the number of gaps longer than 1, 2, 3 etc. ocular scale divisions along the track image.

After determining \bar{G} we calculated the coefficient $g = 1/(\bar{G} + \alpha)$, where $\alpha = 0.28 \mu$ is the average diameter of AgBr crystals. According to O'Ceallaigh¹⁴ g is the density of silver halide crystals which are developable as the result of the passage of a charged particle. We call g the density of developable AgBr grains to distinguish it from n , which is the density of developed Ag grains. In the developing process grain diameter is approximately doubled; one developed grain may appear in place of several closely situated developable AgBr grains. n is thus generally smaller than g .

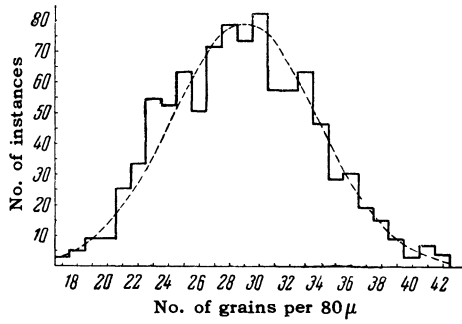


FIG. 2. Distribution of Ag grain density along relativistic electron tracks.

In our R-NIKFI emulsions the average grain density at the ionization plateau was ~ 32 grains per 100μ . Figure 2 shows the grain density distribution n per 80μ along relativistic electron tracks. The χ^2 -test probability P compared with the Gaussian distribution is $P = 0.5$ to 0.6 . The root-mean-square deviation from the mean of grain density along electron tracks is $\sigma = 0.89\sqrt{n}$, which is thus smaller than \sqrt{n} (see reference 15).

In order to determine pair-induced ionization from grain density (n, g) we plotted calibration curves of grain density vs ionization. In the region of single ionization on the plateau (I_{pl}) grain density was measured along electron tracks. The track of a relativistic α particle was used to determine grain density for ionization $4I_{pl}$. In the intermediate region ($2 - 3 I_{pl}$) we used the tracks of a few pions stopping in the emulsion. Pion-induced ionization for different ranges was determined from the curves of Barkas and Young¹⁶ for specific ionization loss in AgBr crystals of Ilford G5 emulsions. The nuclear composition of the R-NIKFI emulsion¹⁷ is close to that of Ilford G5.

Grain density measurements along the tracks of electrons with $\gtrsim 10^9$ ev and of pions with $\sim 5 \times 10^8 - 10^9$ ev gave the following ratio between the grain density n for plateau ionization and the grain density for minimum ionization:

$$n_{pl} / n(I_{min}) = 1.15 \pm 0.03.$$

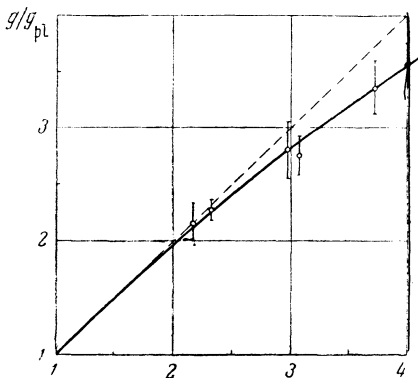


FIG. 4. Developable grain density g as a function of specific ionization loss in AgBr crystals. The dashed line represents $g(I)$ as linear.

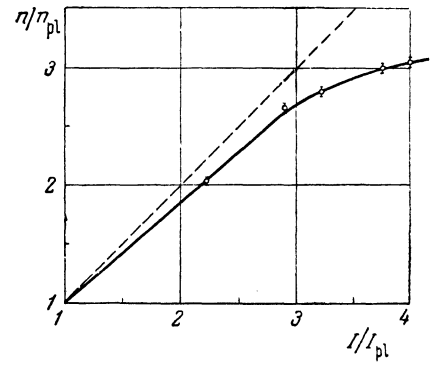


FIG. 3. Grain density n as a function of specific ionization loss in AgBr crystals.

In determining I_{pl} from the known value of I_{min} it was assumed that $I_{pl}/I_{min} \approx n_{pl}/n(I_{min})$. The value used for I_{pl} was $1.01 \text{ Mev cm}^2/\text{g}$.

The calibration curve for the density n of developed grains is shown in Fig. 3 with the statistical errors \sqrt{n} . It is evident from the curve that the grain density $n(2I_{pl})$ of doubly ionizing particles differs from $2n_{pl}$ (dashed curve) representing twice the density of singly ionizing particles by not more than $8 \pm 1\%$.

Figure 4 shows the calibration curve for the density g of developable grains with the errors $g/\sqrt{N_B}$, where N_B is the total number of counted gaps (equal to the number of blobs along the track). The curves show that $g(I)$ is more nearly linear than $n(I)$. The difference between $g(2I_{pl})$ and $2g_{pl}$ does not exceed 1 or 2% .

4. RESULTS

We measured n and g for each of five electron-positron pairs. Figure 5 gives histograms of the measured grain density n for three pairs with $\sim 10^{12}$ ev along 2-mm track segments at the vertex.

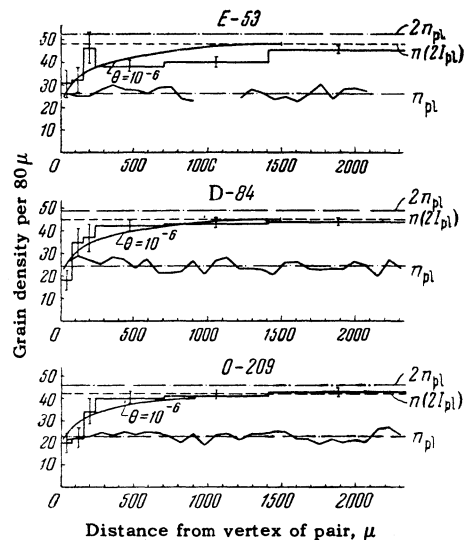


FIG. 5. Grain density n along tracks of pairs with $\sim 10^{12}$ ev (histograms). The irregular line represents the track density for relativistic electrons.

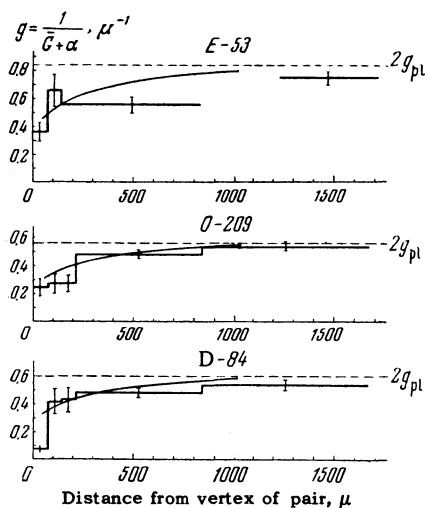


FIG. 6. Density g of developable grains along tracks of pairs with $\sim 10^{12}$ ev.

Statistical errors are indicated, as in all succeeding figures.

The irregular curve at the n_{pl} level serves as an index of the uniformity of emulsion properties and processing for the measured segments; it represents measurements of a few electron tracks at the same depth in the emulsion not farther than 100 or 200 μ from a measured segment of a pair track. Results obtained from different emulsion layers in which a single pair was measured were reduced to a single density n_{pl} . The density g was measured similarly along tracks of pairs (Fig. 6), and the results of the two procedures are seen to agree. In a segment $x < 250 \mu$ at the vertex the observed ionization is clearly less than double ionization. With increase of the distance x from the vertex ionization rises rapidly, but the growth slows down for $x > 250 \mu$. In 1.5–2 mm the grain density along pair tracks approaches the $n(2I_{pl})$ level. Screening evidently occurs here for pairs with $\sim 10^{12}$ ev.

Similar measurements were obtained for two pairs with $\sim 3 \times 10^{11}$ ev (Fig. 7) and, as was to be expected, showed no appreciable reduction of track density at the vertex.

It is interesting to compare our data with Chudakov's calculations,¹ according to which when multiple scattering of electrons is absent pair ionization in an emulsion must obey the law

$$I = 2I_{pl} \frac{23.9 + \ln \theta x}{9.4}, \quad (1)$$

where θ is the vertex angle of the pair in radians

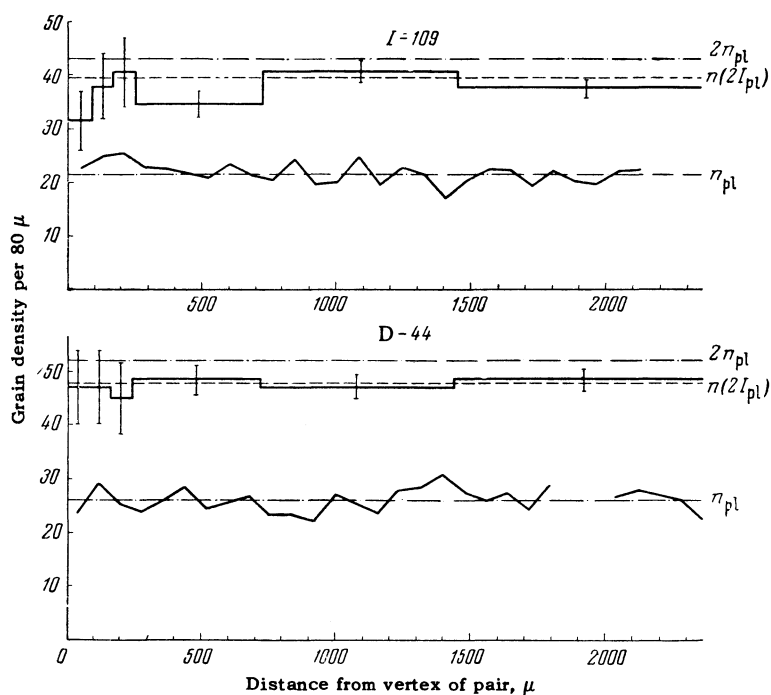


FIG. 7. Grain density n along tracks of pairs with $\sim 3 \times 10^{11}$ ev.

and x is the distance from the vertex in centimeters (4×10^{-11} cm $< \theta \times x \lesssim 3 \times 10^{-7}$ cm).

When multiple scattering is taken into account as in reference 1, but with the correct value of the scattering constant $K = 27\sqrt{\pi}$ Mev \cdot deg/ $\sqrt{100 \mu}$ which gives the spatial separation of two electrons departing from the point $x = 0$ in the same direction the formula becomes

$$I = 2I_{pl} \frac{23.9 + \ln(\theta x \sqrt{1 + 70x})}{9.4}, \quad (2)$$

where θ is the most probable vertex angle.

The best agreement between the experimental results for pairs in D-84, O-209, and E-53 and the theoretical curve (2) was observed for θ close to 10^{-6} . Figures 5 and 6 show the curves of n and g obtained from (2) for $\theta = 10^{-6}$ and the calibration curves. According to Borsellino⁴ the angle $\theta = 10^{-6}$ corresponds to the most probable pair energy $E_\gamma = 2 \times 10^{12}$ ev.

Table II shows that the values of E_γ obtained by the different methods are in agreement, thus confirming the possibility of determining pair energies from ionization by using theoretical formulas which take screening into account. The uncertainty in determining E_γ from the screening effect results from statistical errors in determining ionization, from multiple scattering, the probabilistic character of the relation between θ and E_γ and the inexactitude of the theoretical formula. Additional experimental data are obviously needed to determine the errors in the values of E_γ obtained from ionization.

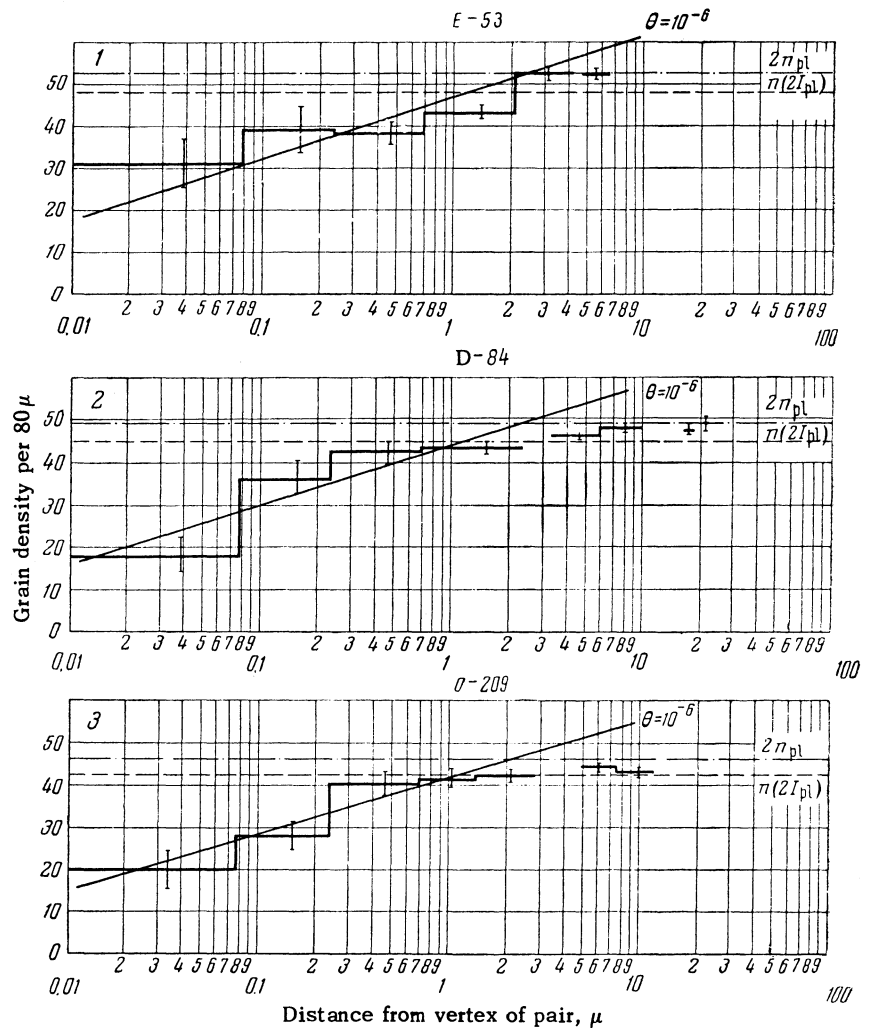


FIG. 8. Grain density n along tracks of pairs with $\sim 10^{12}$ ev.

We have compared our ionization measurements only with formula (2) of Chudakov,¹ which takes multiple scattering into account more correctly than the formula of Yekutieli,² for example. The latter ionization formula for a pair separated by the distance r (in cm) is

$$I = 2I_{pl} \frac{41.5 + \ln(r^2)}{13}.$$

The average of I is obtained by averaging $\ln(r^2)$. Integration of r multiplied by a function of its distribution is performed over the entire region from 0 to ∞ , thus including the region of r where the given formula for I is meaningless ($0 \leq I \leq 2I_{pl}$).

Grain densities n were also measured at large distances x from the vertex (along almost the entire coalesced track segment). Figure 8, which gives the results for three high-energy pairs, shows a gradual increase of n for $x > 1$ or 2 mm, although the specific ionization loss of a pair remains constant.

A study of the structure of shower E-53 shows that one electron of the first pair possesses much

higher energy than the other electron, so that the distance between the paths of the pair members increases more rapidly than in the case of the D-84 and O-209 pairs. This can account for the fact that n approaches the $2n_{pl}$ level more rapidly along the E-53 pair.

It is clear that the growth of grain density from the $n(2I_{pl})$ level to the $2n_{pl}$ level is a purely geometric effect. The $2n_{pl}$ level is reached as the electron separation becomes comparable to the diameter of developed grains ($\sim 5 \times 10^{-5}$ cm), i.e., when the adhesion of grains no longer affects the count. The blob density is even more strongly subject to this geometric effect.

In the present work for a visual count of n the difference $\{2n_{pl} - n(2I_{pl})\}/2n_{pl}$ was 8%, while the corresponding blob difference was about 20%. Weill and his coworkers¹⁸ give 20% as the blob density.

We shall now estimate how much the gap density can be increased by the geometric effect. We first note that in the region where r is greater than or comparable to the diameter of AgBr crys-

tals ($r \gtrsim 2 \times 10^{-5}$ cm) the density g along a pair track remains constant. The gap density b and the average gap G are also constant. Indeed, in the measurement of gaps along a pair track (the x axis), when two grains not separated by a gap along x are taken as a single grain, the size and number of gaps is independent of the grain distribution in the plane perpendicular to the x axis. If when grain diameters are increased during the developing process there is no repulsion between contiguous grains the grain distribution with respect to x along pair tracks will also be independent of r (for constant g).

We shall now consider the region 5×10^{-7} cm $\leq r \leq 2 \times 10^{-5}$ cm. We denote by $\pi(I)$ the probability that a grain is struck during specific ionization loss I . According to reference 19 the gap density b is defined by $b = \pi(1 - \pi)^k$, where k is given approximately by the ratio between the diameters of a developed and undeveloped grain. For the R-NIKFI emulsion we have $k \approx 2$ and $\pi(I_{p1}) = 0.08$.

For distances 5×10^{-7} cm $\lesssim r \ll 2 \times 10^{-5}$ cm the values of b and \bar{G} will be determined by the probability $\pi(2I_{p1})$. On the other hand, for r comparable with the diameter of AgBr crystals ($r \sim 2 \times 10^{-5}$ cm) b and \bar{G} will be determined by the probability $2\pi(I_{p1}) - [\pi(I_{p1})]^2$.

With small recombination we have, generally,

$$\pi(2I) \gtrsim \{2\pi(I) - [\pi(I)]^2\}$$

and b will not increase with r ; there may even be some decrease of b .

The inequality $\pi(2I_{p1}) < \{2\pi(I_{p1}) - [\pi(I_{p1})]^2\}$ can be satisfied if recombination in AgBr grains for double specific losses $2I_{p1}$ is appreciably greater than for I_{p1} .

According to Della Corte et al.²⁰ $\pi(2I_{p1})$ can be reduced by $\sim 3\%$ as a result of recombination, while $\pi(I_{p1})$ can be reduced by $1 - 2\%$. Therefore the greatest possible growth of b through the geometric effect is not above $1 - 2\%$. Thus the geometric effect must be very small for gap density (in the sense of the growth of b), unlike the case for the grain density n and blob density

In principle the geometric effect can also be used to determine the divergence angle of a pair; in this case it is better to use the blob density. The geometric effect will also appear for pairs with lower energies, when screening is absent; but this cannot result in errors when energy is determined from decreased ionization at the vertex since the two effects differ. Screening reduces pair ionization and track density compared with the level for a doubly ionizing particle, while the

geometric effect would increase the density above this level.

We find no grounds for the conclusion reached by Weill, Gailloud, and Rosset¹⁸ that ionization measurements for pairs with energies $\gtrsim 10^{10}$ ev and the use of formulas that take screening into account will increase the result of the geometric effect by a factor of 100. If this were true the geometric effect for 5×10^{-7} cm $\lesssim r \lesssim 2 \times 10^{-5}$ cm could reduce track density compared with the level corresponding to double ionization. Our pairs had a small angle of divergence, so that their components were separated by a small distance for a relatively long time. The investigated region of the geometric effect occupies altogether about 2 cm of pair tracks. This region nowhere showed any appreciable reduction of n or g compared with the double ionization level. This refers particularly to measurements of n and g for the I-109 pair in an Ilford G5 plate. In any event, a reduction below the double ionization level could only be observed at the vertex.

As was stated by Weill et al, in their paper the variation of blob density resulting from the geometric effect is treated as a variation of ionization I ; this led to the conclusion regarding the error in determining E_γ from screening. With calibration curves like those in Figs. 3 and 4 it is always possible to distinguish the regions of the geometric effect and screening.

Our results and those obtained by Perkins and by Wolter and Miesowicz²¹ thus show the possibility of using the screening to determine pair energies. Any track parameters may be used which are sufficiently sensitive to variation of the ionization near $2I_{p1}$. The geometric effect cannot change the ionization and increase the energy E_γ .

In conclusion the authors wish to thank Professor I. I. Gurevich for his interest and for discussions, A. A. Kondrashina for assistance with the treatment of experimental results and D. M. Samoilovich and his group for the developing of the emulsions.

¹ A. E. Chudakov, *Izv. Akad. Nauk SSSR, Ser. Fiz.*, **19**, 651 (1955) (Columbia Tech. Transl. p. 589).

² G. Yekutieli, *Nuovo cimento* **5**, 1381 (1957).

³ I. Mito and H. Ezawa, *Progr. Theoret. Phys.* **18**, 437 (1957).

⁴ A. Borsellino, *Phys. Rev.* **89**, 1023 (1953).

⁵ M. Stearns, *Phys. Rev.* **76**, 836 (1949).

⁶ E. Lohrmann, *Nuovo cimento* **2**, 1029 (1955).

⁷ Varfolomeev, Gerasimova, and Gurevich, *Proceedings of the 1958 Annual International Conference on High Energy Physics at CERN*, 1958, p. 297.

- ⁸ K. Pinkau, *Nuovo cimento* **3**, 1285 (1956).
- ⁹ Miesowicz, Stanisz, and Wolter, *Bull. Acad. Polon. Sci., Cl. III*, **4**, 811 (1956).
- ¹⁰ L. Janossy and H. Messel, *Proc. Roy. Irish Acad.* **A54**, 217 (1956).
- ¹¹ L. Janossy, *Acta Phys. Hung.* **2**, 289 (1952).
- ¹² Varfolomeev, Golenko, and Svetloobov, *Dokl. Akad. Nauk SSSR* **122**, 785 (1958), *Soviet Phys. "Doklady"* **3**, 977 (1958).
- ¹³ P. H. Fowler and D. H. Perkins, *Phil. Mag.* **46**, 587 (1955).
- ¹⁴ C. O'Ceallaigh, *Compt. rend. Congrès de Bagnères*, 1953, p. 73; *Supplemento Nuovo cimento* **12**, 412 (1954).
- ¹⁵ P. E. Hodgson, *Brit. J. Appl. Phys.* **3**, 11 (1952).
- ¹⁶ W. H. Barkas and D. M. Young, *University of California Radiation Laboratory Report UCRL-2579*, Berkeley, Cal., 1954.
- ¹⁷ M. F. Rodicheva, *Журн. науч. и прикл. фотограф. и кинематогр.* (*Journal of Scientific and Applied Photography and Cinematography*) No. 3, 286 (1958).
- ¹⁸ Weill, Gailloud, and Rosselet, *Nuovo cimento* **6**, 1430 (1957).
- ¹⁹ Della Corte, Ramat, and Ronchi, *Nuovo cimento* **10**, 509 (1953).
- ²⁰ Della Corte, Ramat, and Ronchi, *Nuovo cimento* **10**, 958 (1953).
- ²¹ D. H. Perkins, *Phil. Mag.* **46**, 1146 (1955); W. Wolter and M. Miesowicz, *Nuovo cimento* **4**, 648 (1956).

Translated by I. Emin

132